

INVESTIGATION OF CORROSION RESISTANCE OF MIXED ZINC ALUMINUM AND MAGNESIUM COATINGS IN VARYING ACIDIFIED SALINE ENVIRONMENTS

W. Rejmer¹, P. Matyszkiel¹, E. Cieszyńska-Bońkowska², C. Senderowski³

¹University of Warmia and Mazury in Olsztyn, Department of Materials and Machines Technology, Oczapowskiego 11, 10-719 Olsztyn, Poland

²Enzeit Technik, ul. Przejazdowa 21, 05-800 Pruszków, Poland

³Warsaw University of Technology, Institute of Mechanics and Printing, Narbutta 85, 02-524 Warsaw, Poland

ABSTRACT

The increasing drive to use light materials, which will also meet the demands of industry, causes growing interest in zinc mixed coatings. Especially compositions of zinc, aluminum and magnesium are of considerable interest due to their sacrificial protection of coated steel sheet metal in neutral and saline environments. The question that materials experts face is the amount of coating used for anticorrosive protection, as it can significantly lower the cost of large-scale installations. In the presented research, corrosion parameters of commercially available coating with three varying coating masses are assessed. The tests were performed using Linear Polarization Resistance Method, which allows for determination of electrochemical parameters and corrosion wear. The obtained results show that a coating with the most mass does not always provide the most optimal protection in all environments. It is suggested that lower coating masses may lead to more uniform deposition of protective products of electrochemical reactions. Additionally it was found out that thickness of substrate leads to different corrosion protection parameters in same thickness coatings.

KEYWORDS: zinc-magnesium aluminum coatings, electrochemical corrosion, corrosion wear

INTRODUCTION

Corrosive material degradation costs the world economy trillions of dollars. The increase in demand for new materials and their cost is leading to a reassessment of materials testing in this field [1]. Norms for assessment of corrosive resistance of materials often employ testing in neutral environments. However, the increasing acidification of the environment caused by industrial processes and climate change should lead to more considerable testing in higher hydrogen ion concentrations [2]. Increased greenhouse gas emissions will inevitably lead to reductions in the pH of oceanic and intracontinental water environments. It is estimated that within the next two decades, the pH value of seawater will change from 8 to 7 [3, 4]. In addition, polluted industrial environments contain acidic ions, such as SO_4^{2-} , CO_3^{2-} and Cl^- ; these ions originate from industrial effluents and can cause structural failure [5]. It is widely understood that fluid acidity, particularly highly aggressive acidic ions, is critical in the corrosion and degradation of metal alloys [5, 6]. A variety of mechanisms can cause corrosion. Its early stages can benefit further protection by forming dense protective layers on the surface, which can significantly reduce the corrosion rate [7, 8]. Examination of the time-dependent damage processes revealed that a surface corrosion layer can mitigate the influence of tensile stress on the the Ni–Cr–Mo–V [9]. Zinc and other

amphoteric coating materials applied to metallic surfaces are of considerable interest for this reason alone. Various order elements, such as aluminum and magnesium, are also added to improve the anodic properties of zinc [10, 11]. Zinc coating has excellent corrosion resistance and protection against steel corrosion. It has great application prospects in the corrosion protection of iron and steel materials. Its chemical and electrochemical properties lead to the formation of a metal oxide or carbonate layer in the atmosphere, which covers the surface of the alloy and prevents further oxidation. This is due to the fact that the standard potential of zinc is more anodic than the standard potential of iron. Therefore, the galvanized layer with more negative potential will corrode preferentially even when a local breakage occurs. Furthermore, it still has electrochemical protection for steel, sacrificing itself to protect iron-containing substrates. However, environmental changes and the needs of application scenarios impose stringent requirements on the corrosion resistance of Zn coatings. Corrosion experiments on Zn–Al–Mg alloy coating have been widely conducted. Tests at marine test sites revealed that increasing the eutectic content of the coating improved the corrosion resistance. This finding is related to the formation of stable layered double hydroxides. Similar studies under varying atmospheric conditions for up to 6 years showed that mixed zinc–aluminum–magnesium coatings exhibited excellent corrosion resistance with an

average mass loss ratio of around 3 suggesting that their high corrosion resistance is related to the formation of protective corrosion products [12].

To shorten the time of corrosion experiments, Zn alloy coatings are often studied under simulated environmental conditions in the laboratory rather than in conventional atmospheric environments, in which corrosion is slow. Accelerated studies revealed two types of corrosion areas: grey and white coloured. Both contained hydroxyl zinc, but most of the grey regions comprised hydroxyl zinc chloride, while most of the white areas were sparsely packed substances such as zinc carbonate. The inner corrosion products were dense layered double hydroxides which serve a protective role [13]. Other research in accelerated environments investigated the types of corrosion products and percentages of stabilized products in the coating. Those studies proposed that Mg is preferentially corroded in the coating and that the corrosion products buffer the pH and inhibit oxygen reduction [13]. Experimental evidence has been found that zinc-magnesium-aluminium alloy underwent localized corrosion (similar to pitting corrosion) under high pH conditions, indicating that this alloy might not be suitable in such conditions [14]. The research aims to assess coating mass's influence on its electrochemical properties in a mildly acidified saline environment.

MATERIALS AND METHODS

The research material consisted of Zn3.5Al3Mg type coatings produced by ArcelorMittal by the hot-dip galvanizing method [15] on S350GD and S320GD steel substrates of various thicknesses. The investigation focused on three coating types with varying substance weights (310, 430 and 620 g/m²) and different coating thicknesses. The coatings were coated on both sides and were designated ZM-310, ZM-430, and ZM-620. The ZM-310 coating was applied to a steel material measuring 1.5 mm in thickness, while the ZM-430 coating was applied to steel materials measuring 2.5 and 3 mm thick. In contrast, the ZM-620 coating was the sole product manufactured on S320GD steel with a thickness of 3 mm. According to the manufacturer of the tested coatings, the main component is zinc with 3 wt.% magnesium and 3.5 wt.% aluminium. The structure properties and chemical composition of the coating's surface were analyzed with a Quanta FEG 250 scanning microscope integrated with an EDAX x-ray microanalysis detector. Sodium chloride solutions of 0.25, 0.5 and 1M were used for corrosive testing. Such environments are comparable to environments presented in ISO-12944. The first solution is similar to C4-type environments: chemical plants, swimming pools, ship and boat repair yards, industrial areas, and

coastal areas with medium salinity. The second most concentrated solution has corrosion similar to C5 environments: buildings or areas with almost continuous condensation and high pollution, industrial areas with high humidity and aggressive atmosphere. The most concentrated solution gives results similar to C5-M, structures or areas with almost continuous condensation and high pollution, coastal and offshore areas inland with high salinity [16]. Crystalline sodium chloride (99 % weight ratio, Chempur Poland) and buffer solution with a pH value of 6.5 achieved through the use of (Chempur, Poland) were used to prepare a slightly acidic environment. The study consisted of measurements using the Linear Polarization Resistance (LPR) method. To perform the measurement, a degreased sample (ethanol 96 % by volume) should be placed in an electrochemical vessel and connected to a potentiostat-galvanostat (Atlas 1131). The LPR method involves stabilizing the electrochemical system to a fixed potential, lowering its potential by ΔE , and raising it above the stationary potential by the same amount. During the measurement, the results of the sample potential (V) and the density of the flowing current are read (A/m²). The density of the flowing current is related to the amount of corrosion processes occurring on the metal surface. The resulting polarization curve consists of two parts: the anodizing and cathodizing curve. Tafel curves are then drawn to the anodizing and cathodizing curves. The intersection point of the Tafel curves allows the current density and corrosion potential to be read (Figure 1).

Corrosion wear was determined from the corrosion current values based on Faraday's law (1) [2].

$$m = \frac{MIt}{zF}, \quad (1)$$

m — mass of corroded material, g; *M* — molar mass of metal undergoing reaction, g/mol; *z* — amount of

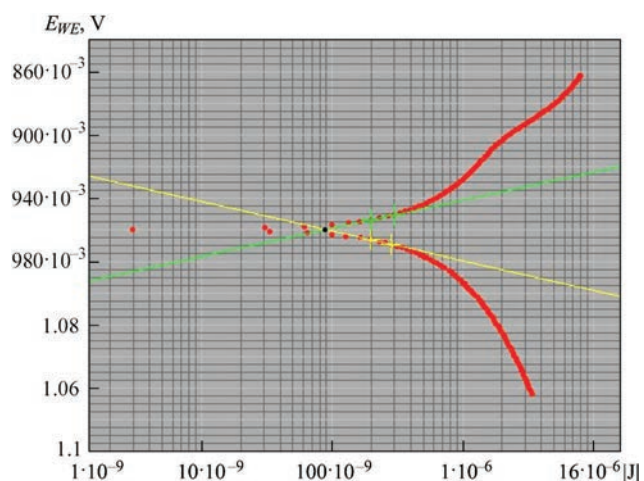


Figure 1. Example of a polarization curve with Tafel tangents

electrons given up in a single oxidation process; F — Faraday's constant 96500, $^{\circ}\text{C/mol}$; I — corrosion current density, A cm^{-2} ; t — time, s.

In order to calculate corrosion wear, the mass percentage composition of the coating was converted to atomic percentage. Subsequently, the molar mass of the alloy was determined to be 59 g/mol. Given that 96.5 % of the coating composition comprises zinc and magnesium, which donate two electrons during the oxidation process, it was assumed that the number of electrons donated per unit process would be 2. To determine the life of the coating, the corrosion potentials of the individual coating components and the amount of coating per square meter of material were used.

RESULTS

SEM ANALYSIS

The SEM/EDS examinations (Figure 2 and Table 1) revealed that two thinner coatings (Figures 2, *a*, *b*) were characterized by a more homogeneous layered structure with numerous material defects in the form of grooves and microcracks with visible grains delamination on the coating surface (Figure 2, *b*). The

coatings structure is formed of elongated grains consisting of the solid solution areas of Al in Zn (α) on a formed eutectic background ($\alpha+\beta$).

It is generally accepted that immersion time and bath temperature influence the cracking and delamination of the primary diffusion layer at the interface with the steel substrate material. However, forming brittle intermetallic phases from the Fe-Al system due to the diffusion of iron from the steel substrate plays a significant role in the delamination of the structure of thin coatings in this zone [17]. A SEM/EDS study of the chemical composition in micro-areas allowed to establish that the most probable phase forming the diffusion layer in the interface with the steel substrate is the $\text{FeAl}_3(\text{Zn})$, which in the final stage of structure formation transforms, creating micro-areas with the participation of even more brittle $\text{Fe}_2\text{Al}_5(\text{Zn})$ phase. This causing microcracks and delamination of layers, as visible in the structure of the ZM-430 coating (Figure 2, *b*). The structure of the same ZM-430 coating on 3 mm thick S350GD steel shows the influence of the steel substrate on the formation of a layer with a high degree of surface development (Figure 2, *c*). Most likely, this effect is due to the high residual stresses that arise from the differing linear coefficients of

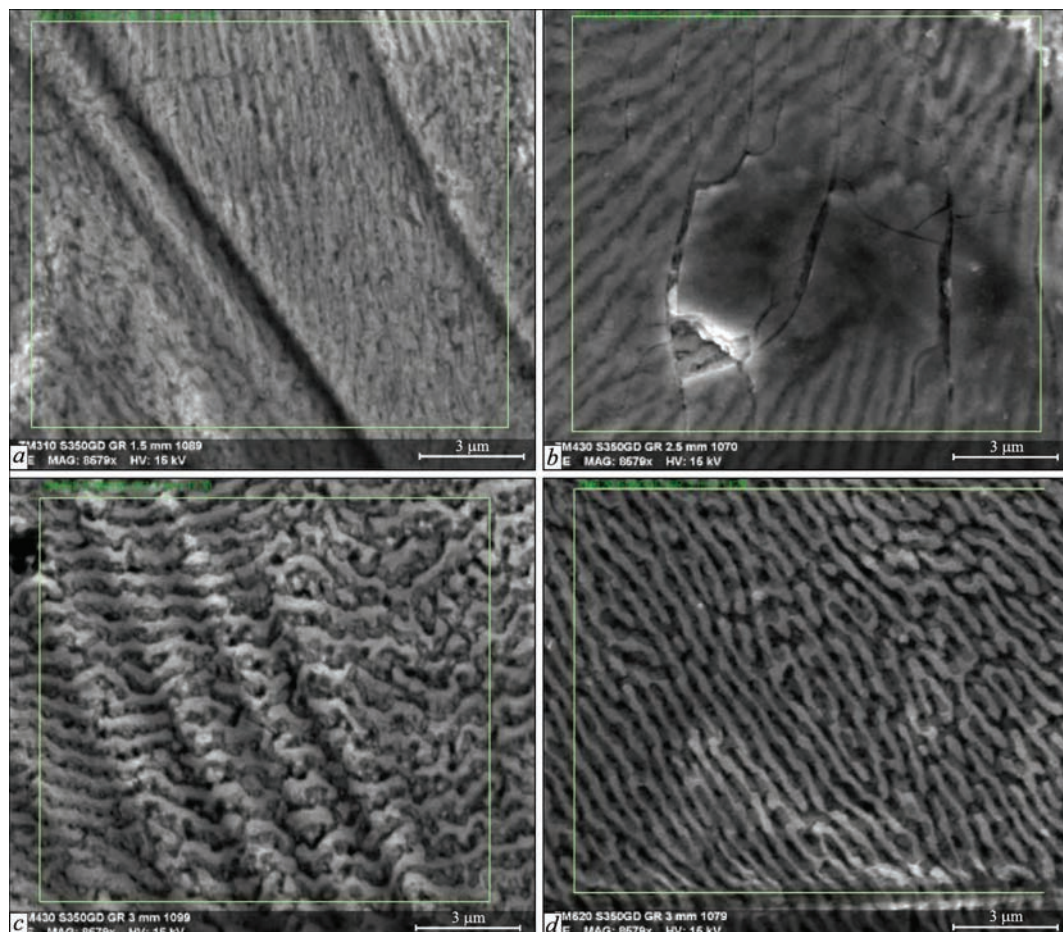


Figure 2. Example SEM/ SE images for: ZM-310 — on 1.5 mm steel (*a*); ZM-430 — on 2.5 mm (*b*) and 3 mm steel (*c*), respectively; and ZM 620 — on 3 mm steel (*d*)

thermal expansion between the steel substrate and the complex, heterogeneous structure of the Zn–Al–Mg coating, which contains high-aluminium intermetallic phases from the Fe–Al system. Studies of Zn–Mg–Al alloy coatings have shown that one of the causes of crack formation is the tensile stresses within the structure, primarily generated by an increased cooling rate [18]. Depending on the thickness of the substrate material and the obtained coating, this phenomenon can influence the proportion of micro-cracks and the microstructural characteristics of the tested coatings. This effect can be observed for ZM-430 coatings of the same weight applied to S350GD steel substrate with different thicknesses of 2.5 and 3 mm. Analysis of the obtained results shows a favourable effect of grain growth kinetics on the structure formation of the ZM-620 coating, produced in a hot dip bath on 3 mm thick S320GD steel. By increasing the thickness of the coating, the rate of the Fe–Al reaction and the formation of brittle intermetallic phases are eliminated, resulting in a more structurally uniform coating in the surface area with no visible material defects (Figure 2, *d*). Microanalysis of the chemical composition on the surface of the ZM-620 coating shows similar amounts of magnesium as indicated by the manufacturer. It has also been found that as the mass (thickness) of the coating increases, the percentage of alloying elements decreases and the carbon and oxygen content increases (Table 1). The formation of carbonate layers, also

Table 1. Semiquantitative EDS analysis of coatings surfaces

Element	ZM-310 1.5 mm		ZM-430 2.5 mm	
	wt.%	at.%	wt.%	at.%
Zinc	82.22±0.56	55.52±0.92	80.44±4.24	52.79±7.07
Oxygen	5.62±0.06	15.52±0.33	6.60±2.33	17.33±5.13
Carbon	4.24±0.38	15.58±1.25	4.8±0.77	16.95±1.55
Aluminum	4.47±0.1	7.31±0.24	4.30±0.44	6.79±0.52
Magnesium	3.28±0.06	5.90±0.05	2.96±0.09	5.21±0.31
Chromium	0.2±0.35	0.17±0.29	0.5±0.53	0.39±0.34
Phosphorus	0	0	0.4±0.36	0.53±0.47

Table 1. Cont.

Element	ZM-430 3 mm		ZM-620 3 mm	
	wt.%	at.%	wt.%	at.%
Zinc	80.88±2.68	52.86±4.09	77.15±3.42	46.83±4.93
Oxygen	5.50±1.64	14.56±3.58	8.56±2.10	20.99±4.13
Carbon	5.45±0.43	19.33±0.87	6.32±0.66	20.78±1.20
Aluminum	4.6±0.19	7.28±0.57	3.91±0.21	5.74±0.41
Magnesium	3.17±0.1	5.56±0.09	2.66±0.32	4.34±0.61
Chromium	0.22±0.39	0.17±0.3	0.85±0.27	0.64±0.18
Phosphorus	0.18±0.31	0.23±0.4	0.53±0.46	0.68±0.59

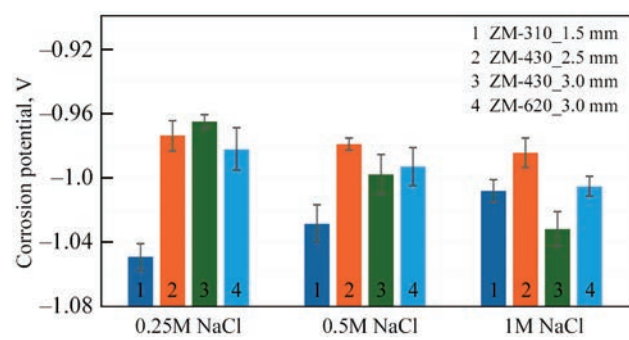


Figure 3. Average values of corrosion potentials

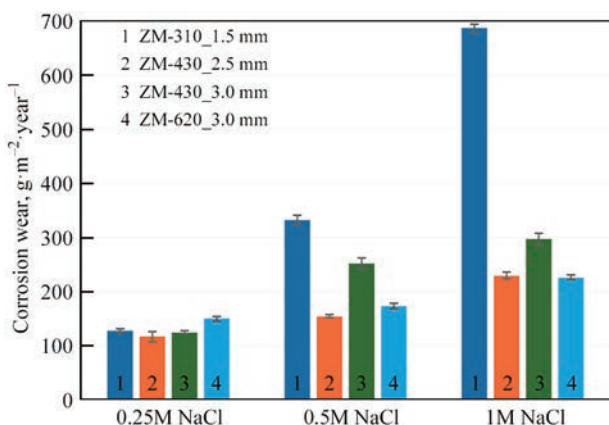
found in [19], is most likely responsible for this. Carbonates form an oxidised protective layer but, unfortunately, are also thought to be permeable to acidic environments.

LPR ANALYSIS

Corrosion potential results are presented in Figure 3 and Table 2. Except for the ZM-310 coating, every other coating has exhibited the highest corrosion potential values in 0.25 M NaCl. The ZM-310 coating showed the lowest corrosion potential in this solution, -1.05 ± 0.01 V. In the least saline solution, the 3 mm thick samples coated with ZM-430 coatings showed the highest average potentials (-0.97 ± 0.009 V), but in most saline solutions, gave the lowest potentials (-1.03 ± 0.01 V). The differences between potentials are minor and can be assumed to be the same. In higher salinity solutions, the highest potential was measured for the ZM-430 coating on 2.5 mm steel substrate (0.98 ± 0.01 V in both solutions). It is worth noting that this coating exhibits the least variation in potential when salinity conditions are changed. This

Table 2. Results of corrosion potentials

Coating, mm	Corrosion potential, V			
	Measure- ment 1	Measure- ment 2	Measure- ment 3	Measure- ment 4
0.25 M NaCl				
ZM310_1.5	-1.05	-1.06	-1.05	-1.04
ZM430_2.5	-0.99	-0.97	-0.97	-0.97
ZM430_3	-0.97	-0.96	-0.97	-0.96
ZM620_3	-1.00	-0.98	-0.97	-0.98
0.5 M NaCl				
ZM310_1.5	-1.03	-1.04	-1.03	-1.02
ZM430_2.5	-0.98	-0.97	-0.98	-0.98
ZM430_3	-0.99	-0.99	-1.00	-1.01
ZM620_3	-1.01	-0.98	-0.99	-0.99
1 M NaCl				
ZM310_1.5	-1.01	-1.02	-1.01	-1.00
ZM430_2.5	-0.98	-0.97	-0.99	-0.99
ZM430_3	-1.02	-1.04	-1.03	-1.04
ZM620_3	-1.00	-1.01	-1.01	-1.00

**Figure 4.** Coating corrosion wear

may be attributed to the high oxygen content in the coating, possibly resulting from protective oxide layers [20]. The ZM 310 coating is predominantly zinc and aluminium rich in the surface layer, which, due to the lowest anodic potential of these metals, may cause a potential increase with increasing salinity [21].

In all of the investigated environments, the lowest average corrosion wear in 0.25 M and 0.5 M NaCl is exhibited by the ZM-430 coating on steel with a thickness of 2.5 mm, which amounts to $115.6 \pm 9.34 \text{ g} \cdot \text{m}^{-2} \cdot \text{year}^{-1}$, $153.31 \pm 2.31 \text{ g} \cdot \text{m}^{-2} \cdot \text{year}^{-1}$, respectively. In most saline solution, the most minor corrosion wear is exhibited by ZM-620 coating ($225.26 \pm 4.62 \text{ g} \cdot \text{m}^{-2} \cdot \text{year}^{-1}$). In 0.25 M NaCl environment, the ZM-620 coating showed the highest corrosion wear ($148.81 \pm 4.39 \text{ g} \cdot \text{m}^{-2} \cdot \text{year}^{-1}$). In higher salinity corrosive environments, the highest corrosion wear for coating ZM-310 was calculated to be $331.31 \pm 8.90 \text{ g} \cdot \text{m}^{-2} \cdot \text{year}^{-1}$ for 0.5 M environment and $687.12 \pm 7.93 \text{ g} \cdot \text{m}^{-2} \cdot \text{year}^{-1}$ for 1 M NaCl (Table 3). During corrosion tests in 1M NaCl solution sample ZM-310 exhibited orange coloring of solution. This observation is probably caused by coating penetration and resulting presence of iron salts in the solution. Additionally the corrosion products of other samples exhibited a white-gray color while ZM-310 sample exhibited black corrosion products, which may be composed of non soluble Fe^{2+} and Fe^{3+} salts. Both of these observations can be related to coating penetration.

The average corrosion wear values are shown in Figure 4, while results from singular measurements are shown in Table 3. Corrosion wear seems to be dependent on coating mass, but not directly. In lower salinity solutions, the most densely coated sample (with ZM-620 coating) shows higher corrosion wear values, which increase less with increasing salinity. It can be assumed that ZM-620 coating is more effective in creating other protective layers due to the

Table 3. Corrosion wear of coatings

Coating	Corrosion wear, $\text{g} \cdot \text{m}^{-2} \cdot \text{year}^{-1}$			
	Measure- ment 1	Measure- ment 2	Measure- ment 3	Measure- ment 4
0.25 M NaCl				
ZM-310, 1.5 mm	131.20	121.07	126.86	126.86
ZM-430, 2.5 mm	123.97	108.05	123.48	107.08
ZM-430, 3 mm	124.93	123.97	119.62	126.38
ZM-620, 3 mm	150.98	143.26	147.60	153.39
0.5 M NaCl				
ZM-310, 1.5 mm	320.29	337.36	328.00	339.58
ZM-430, 2.5 mm	150.50	152.91	155.32	155.32
ZM-430, 3 mm	258.54	236.35	260.47	249.86
ZM-620, 3 mm	171.72	164.97	174.61	176.54
1 M NaCl				
ZM-310, 1.5 mm	686.88	685.91	678.19	697.49
ZM-430, 2.5 mm	228.64	225.74	237.32	223.81
ZM-430, 3 mm	288.45	299.06	289.41	310.64
ZM-620, 3 mm	224.78	218.99	227.67	229.60

high carbon content associated with carbonate salts, and hydroxides layered [21].

CONCLUSIONS

Amount of coating used on steel sheet determines to some extent its corrosion properties. However the highest amount of coating does not always lead to higher potentials and lower corrosion wear. It may be suggested that deposition of substances to top of the coating can be more beneficial in materials with lower coating content. Coating ZM-430 dipped onto 2.5 mm steel sheet exhibits smaller corrosion wear and higher corrosion potentials in some environments than ZM-610 and ZM-430 on thicker steel sheets which can be attributed to different cooling rates.

ACKNOWLEDGEMENT

This research has been done thanks to Enzeit Technik GTV Poland

REFERENCES

1. Ossai, C.I., Boswell, B., Davies, I.J. (2015) Pipeline failures in corrosive environments — A conceptual analysis of trends and effects. *Eng. Failure Analysis*, **53**, 36–58. DOI: <https://doi.org/10.1016/j.engfailanal.2015.03.004>
2. Senderowski, C., Rejmer, W., Vigiliantska, N., Jeznach, A. (2024) Changes in corrosion behaviour of zinc and aluminium coatings with increasing seawater acidification. *Materials*, **17**(3), 536. DOI: <https://doi.org/10.3390/ma17030536>
3. Hao, X., Ruihong, Y., Zhuangzhuang, Z. et al. (2021) Greenhouse gas emissions from the water-air interface of a grassland river: A case study of the Xilin River. *Sci. Rep.*, **11**, 2659. DOI: <https://doi.org/10.1038/s41598-021-81658-x>
4. Chen, C.T.A., Lui, H.K., Hsieh, C.H. et al. (2017) Deep oceans may acidify faster than anticipated due to global warming. *Na-*

ture Clim. Change, **7**, 890–894. DOI: <https://doi.org/10.1038/s41558-017-0003-y>

5. Xu, Y. Huang, Y. Cai, F. Lu, D. Wang X. (2022) Study on corrosion behavior and mechanism of AISI 4135 steel in marine environments based on field exposure experiment. *Sci. of the Total Environment*, **830**, 154864. DOI: <https://doi.org/10.1016/j.scitotenv.2022.154864>

6. Hao, W. Liu, Z. Wu, W.X. Li, Cuiwei Du, Zhang, D. (2017) Electrochemical characterization and stress corrosion cracking of E690 high strength steel in wet-dry cyclic marine environments. *Materials Sci. and Eng.: A*, **710**, 318–328. DOI: <https://doi.org/10.1016/j.msea.2017.10.042>

7. Song, Y. Liu, R. Cui, Y. Meng, F. Liu, L. Wang, F. (2023) Corrosion of high-strength steel in 3.5 % NaCl solution under hydrostatic pressure: Initial corrosion with tensile stress coupling. *Corrosion Sci.*, **219**, 111229. DOI: <https://doi.org/10.1016/j.corsci.2023.111229>

8. LeBozec, N. Thierry, D. Persson, D. Riener, C.K. Luckeneder, G. (2019) Influence of microstructure of zinc-aluminum-magnesium alloy coated steel on the corrosion behavior in outdoor marine atmosphere. *Surface and Coatings Technology*, **374**, 897–909. DOI: <https://doi.org/10.1016/j.surfcoat.2019.06.052>

9. Huanhuan Wei, Yiqun Tang, Chen Chen, Peifeng Xi, (2024) Corrosion behavior and microstructure analysis of butt welds of Q690 high strength steel in simulated marine environment. *J. of Building Eng.*, **84**, 108509. DOI: <https://doi.org/10.1016/j.jobe.2024.108509>

10. Dolgikh, O., Simillion, H., Lamaka, S.V. et al. (2019) Corrosion protection of steel cut-edges by hot-dip galvanized Al(Zn, Mg) coatings in 1 wt.% NaCl: Pt I. Experimental study. *Materials and Corrosion*, **70**, 768–779. DOI: <https://doi.org/10.1002/maco.201810209>

11. Predko, P., Rajnovic, D., Grilli, M.L. et al. (2021) Promising methods for corrosion protection of magnesium alloys in the case of Mg–Al, Mg–Mn–Ce and Mg–Zn–Zr: A recent progress review. *Metals*, **11**(7), 1133. DOI: <https://doi.org/10.3390/met11071133>

12. Thierry, D., Persson, D., LeBozec, N. (2024) Long-term atmospheric corrosion rates of Zn55 Al-coated steel. *Mat. Corros.*, **75**, 694–704. DOI: <https://doi.org/10.1002/maco.202314209>

13. Schürz, S., Luckeneder, G.H., Fleischanderl, M. et al. (2010) Chemistry of corrosion products on Zn–Al–Mg alloy coated steel. *Corrosion Sci.*, **52**. DOI: <https://doi.org/10.1016/j.corsci.2010.05.044>

14. Romina Krieg et al. (2014) Corrosion of zinc and Zn–Mg alloys with varying microstructures and magnesium contents. *J. Electrochem. Soc.*, **161**, C156. DOI: <https://doi.org/10.1149/2.103403jes>

15. https://industry.arcelormittal.com/industry/repository/fce/Brochures/Magnelis_book_EN.pdf (available at 11.10.2024)

16. ISO 12944

17. Kania, H. (2017) *Structure shaping and corrosion resistance of Zn–Al coatings obtained in hot dip metallization*. Gliwice, Silesian University of Technology.

18. Jihun Choi, Eui-Jin Jung, Dong-Jae Park et al. (2024) Impact of cooling rates on the microstructure and cracking susceptibility of hot-dip galvanized Zn–12 wt.% Al–5 wt.% Mg coatings. *Surf. and Coat. Technol.*, **488**, 131050. DOI: <https://doi.org/10.1016/j.surfcoat.2024.131050>

19. Prosek, T., Larché, N., Vlot, M. et al. (2010) Corrosion performance of Zn–Al–Mg coatings in open and confined zones in conditions simulating automotive applications. *Materials and Corrosion*, **61**, 412–420. DOI: <https://doi.org/10.1002/maco.200905425>

20. Zaid, B., Saidi, D., Benzaid, A., Hadji, S. (2008) Effects of pH and chloride concentration on pitting corrosion of AA6061 aluminum alloy. *Corrosion Sci.*, **50**, 1841–1847. DOI: <https://doi.org/10.1016/j.corsci.2008.03.006>

21. Martin, A., Texier-Mandoki, N., Crusset, D. et al. Corrosion behavior and sacrificial properties of Zn and Zn–Al coatings in conditions simulating deep geological disposal of radioactive waste at 80 °C. *Coatings*, **12**(8), 1044. DOI: <https://doi.org/10.3390/coatings12081044>

ORCID

W. Rejmer: 0000-0002-1955-1553

C. Senderowski: 0000-0001-9584-3139

CONFLICT OF INTEREST

The Authors declare no conflict of interest

CORRESPONDING AUTHOR

W. Rejmer

University of Warmia and Mazury in Olsztyn,
Department of Materials and Machines Technology,
Oczapowskiego 11, 10-719 Olsztyn, Poland.E-mail: wojciech.rejmer@uwm.edu.pl**SUGGESTED CITATION**W. Rejmer, P. Matyszkiel,
E. Cieszyńska-Bońkowska², C. Senderowski
(2024) Investigation of corrosion resistance of mixed
zinc aluminum and magnesium coatings in varying
acidified saline environments. *The Paton Welding J.*,
11, 14–19.DOI: <https://doi.org/10.37434/tpwj2024.11.02>**JOURNAL HOME PAGE**<https://patonpublishinghouse.com/eng/journals/tpwj>

Received: 10.09.2024

Received in revised form: 28.10.2024

Accepted: 06.12.2024

The Paton Welding Journal

SUBSCRIBE TODAY

Available in print (348 Euro) and digital (288 Euro) formats

patonpublishinghouse@gmail.com; journal@paton.kiev.ua<https://patonpublishinghouse.com>